

Supplemental data

Table S1, related to Figure 1

siRNA library. Provided as an Excel file.

Table S2, related to Figure 1: Genes for which siRNA significantly decreased nuclei number (NN), significantly increased neurite length (NL), or both.

Significantly affected genes in SY5Y

gene	NN	NN z score	NL	NL z score	Affected process
CENPE	0.47	-4.30			proliferation
INCENP	0.48	-4.19			proliferation
CTCF	0.65	-2.61			proliferation
JMJD2B	0.66	-2.52			proliferation
HMGN1	0.66	-2.51			proliferation
SUV420h1	0.67	-2.39			proliferation
H2AFX	0.68	-2.32			proliferation
SETD8	0.70	-2.14			proliferation
BC-2	0.70	-2.14			proliferation
ACTR5	0.70	-2.13			proliferation
CHD4	0.70	-2.06			proliferation
HTATIP	0.71	-1.99			proliferation
KIAA0892	0.71	-1.97			proliferation
ATF2	0.72	-1.91			proliferation
RAD21	0.72	-1.89			proliferation
MEN1	0.73	-1.86			proliferation
TNP2	0.73	-1.86			proliferation
CBX1	0.74	-1.76			proliferation
BRD4	0.74	-1.75			proliferation
HMGN4	0.74	-1.75			proliferation
RBM10	0.74	-1.74			proliferation
BAZ1B	0.75	-1.64			proliferation
POGZ	0.75	-1.64			proliferation
FLI1	0.75	-1.59			proliferation
EHMT2	0.76	-1.55			proliferation
MYST1	0.76	-1.52			proliferation
CITED2	0.76	-1.51			proliferation
HRMT1L2	0.77	-1.46			proliferation
SMARCB1			1.78	3.33	differentiation
CENPE			1.73	3.07	differentiation
HMGN4			1.66	2.72	differentiation
CTCF			1.65	2.66	differentiation
SMARCE1			1.64	2.59	differentiation
INCENP			1.63	2.58	differentiation
VCX			1.62	2.53	differentiation
EED			1.60	2.44	differentiation
TADA2L			1.59	2.39	differentiation
ATAD2			1.57	2.25	differentiation
ARID1B			1.55	2.18	differentiation
SETD8			1.55	2.16	differentiation
POLE3			1.52	2.03	differentiation
BAP1			1.52	2.02	differentiation
HMGN1			1.51	1.95	differentiation
CHRAC1			1.51	1.95	differentiation
MSH6			1.50	1.91	differentiation
HBXAP			1.49	1.85	differentiation
FBXL11			1.48	1.82	differentiation
CENPE	0.47	-4.30	1.73	3.07	both
INCENP	0.48	-4.19	1.63	2.58	both
CTCF	0.65	-2.61	1.65	2.66	both
HMGN1	0.66	-2.51	1.51	1.95	both
SETD8	0.70	-2.14	1.55	2.16	both
HMGN4	0.74	-1.75	1.66	2.72	both

Significantly affected genes in BE2C

gene	NN	NN z score	NL	NL z score	Affected process
BC-2	0.59	-3.17			proliferation
CENPE	0.59	-3.14			proliferation
RAD21	0.60	-3.05			proliferation
JMJD2B	0.62	-2.86			proliferation
CHAF1A	0.62	-2.85			proliferation
RAN	0.64	-2.72			proliferation
BRD4	0.66	-2.54			proliferation
KLHDC3	0.66	-2.50			proliferation
KIAA0892	0.70	-2.17			proliferation
ZBTB33	0.70	-2.16			proliferation
HIST3H3	0.70	-2.13			proliferation
TNP2	0.72	-1.97			proliferation
TAF6L	0.73	-1.93			proliferation
PRKCB1	0.73	-1.90			proliferation
TRIM28	0.73	-1.87			proliferation
CENPF	0.73	-1.85			proliferation
ACTR5	0.73	-1.85			proliferation
POU5F1	0.74	-1.83			proliferation
FLJ32440	0.74	-1.81			proliferation
H2AFX	0.74	-1.80			proliferation
MBD1	0.75	-1.76			proliferation
BRD2	0.75	-1.70			proliferation
BCOR	0.76	-1.66			proliferation
NFRKB	0.76	-1.66			proliferation
CENPA	0.76	-1.58			proliferation
RAG2	0.77	-1.58			proliferation
CARM1	0.77	-1.56			proliferation
SMARCA4	0.77	-1.56			proliferation
ATM	0.77	-1.55			proliferation
EHMT2	0.77	-1.52			proliferation
HMG20B	0.78	-1.47			proliferation
EZH2	0.78	-1.45			proliferation
SIRT7	0.78	-1.44			proliferation
PRDM2	0.78	-1.42			proliferation
CBX2	0.79	-1.39			proliferation
PCGF6	0.80	-1.27			proliferation
SETD8	0.80	-1.05			proliferation
C21ORF107			2.53	6.28	differentiation
TNP2			1.80	3.34	differentiation
SUPT6H			1.76	3.20	differentiation
EZH2			1.70	2.97	differentiation
JMJD2B			1.69	2.90	differentiation
POGZ			1.52	2.24	differentiation
GF11B			1.51	2.18	differentiation
BRD4			1.49	2.11	differentiation
CENPE			1.48	2.09	differentiation
TAPBP			1.47	2.05	differentiation
SMC1L1			1.45	1.97	differentiation
RAG2			1.45	1.96	differentiation
ACTR5			1.44	1.93	differentiation
SMARCA1			1.44	1.92	differentiation
HDAC6			1.44	1.92	differentiation
CHAF1A			1.43	1.89	differentiation
BRD2			1.41	1.81	differentiation
TBL1XR1			1.41	1.80	differentiation
CHRAC1			1.40	1.77	differentiation
SMARCB1			1.40	1.77	differentiation
PRDM2			1.39	1.72	differentiation
JMJD2A			1.39	1.72	differentiation
UCHL5			1.38	1.68	differentiation
TAF6L			1.36	1.60	differentiation
CENPE	0.59	-3.14	1.48	2.09	both
JMJD2B	0.62	-2.86	1.69	2.90	both
CHAF1A	0.62	-2.85	1.43	1.89	both
BRD4	0.66	-2.54	1.49	2.11	both
TNP2	0.72	-1.97	1.80	3.34	both
TAF6L	0.73	-1.93	1.36	1.60	both
ACTR5	0.73	-1.85	1.44	1.93	both
BRD2	0.75	-1.70	1.41	1.81	both
RAG2	0.77	-1.58	1.45	1.96	both
EZH2	0.78	-1.45	1.70	2.97	both
PRDM2	0.78	-1.42	1.39	1.72	both

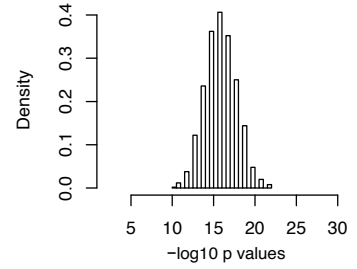
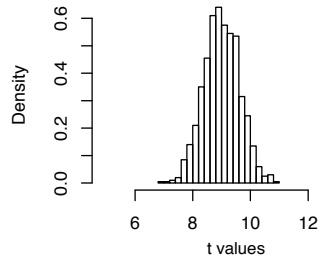
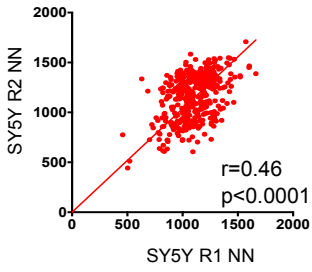
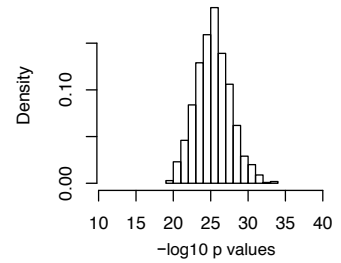
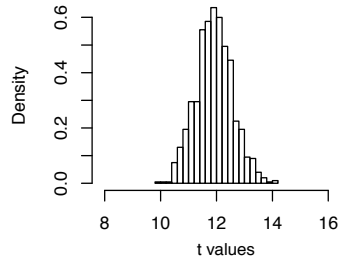
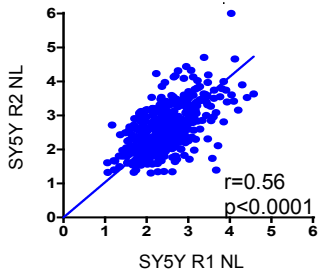
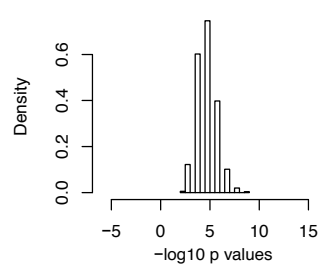
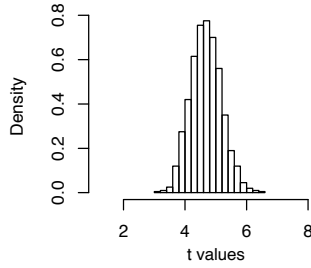
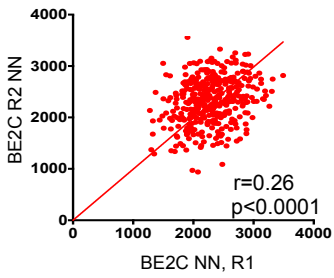
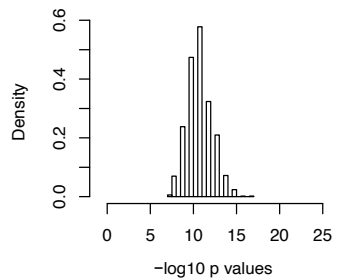
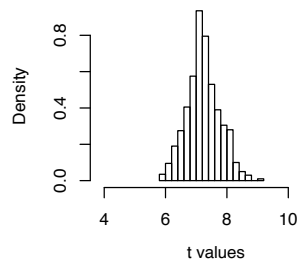
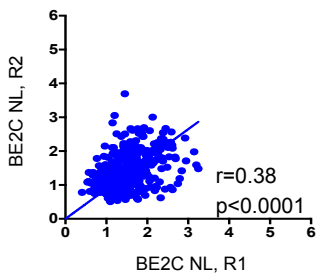
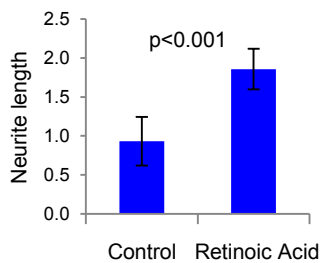
A**B****C****D****E**

Figure S1, related to Figure 1**Measures of the high-throughput RNAi screening reproducibility**

Scatter plots and permutation tests provide measures of assay reproducibility between biological replicates for the measured quantities of nuclei number (NN) and neurite length (NL) for SY5Y and BE2C cells. For each comparison, a permutation test was performed using the linear model function in R with resampling of 300 genes from the data 1000 times. (A) Scatter plot of NN for SY5Y for two biological replicates, R1 and R2. Pearson correlation coefficient and relative p value for Pearson correlation are indicated (left). The distribution of t values for SY5Y NN replicates has a mean \pm SD of 9.0 ± 0.62 (middle graph). The distribution of $-\log_{10}$ p values for SY5Y NN replicates has a mean \pm SD of 16.1 ± 1.95 (right graph). (B) Scatter plot of NL for SY5Y for two biological replicates, R1 and R2. Pearson correlation coefficient and relative p value for Pearson correlation are indicated (left). The distribution of t values for SY5Y NL has a mean \pm SD of 11.9 ± 0.66 (middle graph). The distribution of $-\log_{10}$ p values for SY5Y NL has a mean \pm SD of 25.84 ± 2.33 (right graph). (C) Scatter plot of NN for BE2C for two biological replicates, R1 and R2. Pearson correlation coefficient and relative p value for Pearson correlation are indicated (left). The distribution of t values for BE2C NN has a mean \pm SD of 4.68 ± 0.50 (middle graph). The distribution of $-\log_{10}$ p values for BE2C NN has a mean \pm SD of 4.9 ± 1.04 (right graph). (D) Scatter plot of NL for BE2C for two biological replicates, R1 and R2. Pearson correlation coefficient and relative p value for Pearson correlation are indicated (left). The distribution of t values for BE2C NL has a mean \pm SD of 7.24 ± 0.54 (middle graph). The distribution of $-\log_{10}$ p values for BE2C NL has a mean \pm SD of 10.95 ± 1.49 (right graph). (E) Neurite length in SY5Y cells treated with vehicle or 5 μ M Retinoic acid for 72 hr, measured by the Opera microscope. Bars represent the average of three replicates \pm SD ($p < 0.0001$).

Table S3, related to Figure 1

Statistically significant genes for which at least 50% of the deconvoluted siRNAs decreased nuclei number (NN) and increased neurite length (NL) in SY5Y. Provided as an Excel file.

Table S4, related to Figure 2: Average IC50 (μM) of the 21 epigenetic compounds in MYCN wt and amplified NB cells compared with control cells.

DrugName	Target	Mean											Mean MYCN wt	Mean MYCN Amp	p-value control vs. NB	IVTI
		IC ₅₀ (μM), NB	NBEB	NBLS	SK-N-AS	SY5Y	IMR32	SK-N-BE2C	KCNR	NGP	HEK 293T	ARPE-19				
UNC0379	SETD8	2.05	2.12	3.19	1.30	1.37	2.59	4.20	0.95	0.65	9.16	9.58	2.00	2.10	4E-05	4.58
UNC1999	EZH1/2	5.25	4.43	8.21	5.36	3.92	6.76	3.72	3.72	5.87	10.55	16.71	5.48	5.02	1E-03	2.60
Bromosporin	panBromo	1.28	0.00	0.26	1.87	1.30	1.80	0.95	2.49	1.56	3.85	12.64	0.85	1.70	5E-03	6.46
UNC0638	KMT1C	2.92	4.21	7.08	2.71	1.79	2.84	0.13	1.29	3.35	7.78	8.44	3.95	1.90	1E-02	2.77
JQ1-S	BRD4	0.11	0.21	0.03	0.34	0.15	0.12	0.03	0.03	0.01	6.33	96.65	0.18	0.05	2E-02	448.59
SGC-CBP30	CREBBP	7.16	8.80	1.45	14.09	1.43	0.90	17.37	1.09	12.18	15.06	100.0	6.44	7.88	2E-02	8.03
SAHA	HDAC1	0.52	0.43	0.77	0.42	0.43	0.76	0.43	0.23	0.68	1.99	100.0	0.51	0.52	3E-02	98.49
Cpd50	panKDM	0.23	0.33	0.04	0.05	0.12	0.06	0.98	0.00	0.30	0.54	1.55	0.13	0.33	3E-02	4.47
GSK-J4	JMJD3	0.59	0.75	0.12	0.78	0.50	0.38	0.93	0.35	0.93	1.50	100.0	0.54	0.65	3E-02	85.64
LSD-690	LSD1	36.92	30.62	100.0	19.83	12.28	63.18	9.66	30.70	29.09	66.38	100.0	40.68	33.16	8E-02	2.25
OJI-1	HDAC8	13.05	5.97	26.92	13.08	4.40	5.22	19.85	4.86	24.12	18.80	27.68	12.59	13.51	2E-01	1.78
MC1568	HDAC4	28.94	100	100.0	2.03	4.14	17.09	1.04	0.86	6.36	54.31	100.0	51.54	6.34	2E-01	2.67
Merck60	HDAC1	15.94	16.50	100.0	2.62	1.00	5.13	1.06	1.05	0.20	16.70	100.0	30.03	1.86	2E-01	3.66
GSK343	EZH2	10.04	12.89	27.69	6.89	7.30	11.34	8.77	3.35	2.11	12.29	24.50	13.69	6.39	2E-01	1.83
PFI-2	SETD7	73.78	100.0	100.0	100.0	32.51	31.06	100.0	26.64	100.0	100.0	100.0	83.13	64.43	4E-01	1.36
WT161	HDAC6	3.55	1.03	8.98	1.59	2.55	4.11	4.06	1.06	5.02	5.81	4.11	3.54	3.56	5E-01	1.40
SGC0946	DOT1L	49.24	100.0	10.69	34.43	11.38	27.76	100.0	9.67	100.0	29.52	28.05	39.13	59.36	5E-01	0.58
PFI-3	SMARCA4	89.91	100.0	100.0	82.34	48.76	88.16	100.0	100.0	100.0	100.0	90.33	82.78	97.04	7E-01	1.06
EX527	SIRT1	74.60	100.0	100.0	36.35	35.47	82.96	100.0	100.0	42.03	83.92	48.18	67.96	81.25	7E-01	0.89
LLY-507	SMYD2	14.69	3.24	4.25	2.04	1.32	2.86	0.84	100.0	2.94	4.43	9.40	2.71	26.66	8E-01	0.47
GSK2801	BAZ2A	78.18	100.0	100.0	100.0	20.85	46.82	100.0	100.0	57.75	64.74	84.40	80.21	76.14	9E-01	0.95

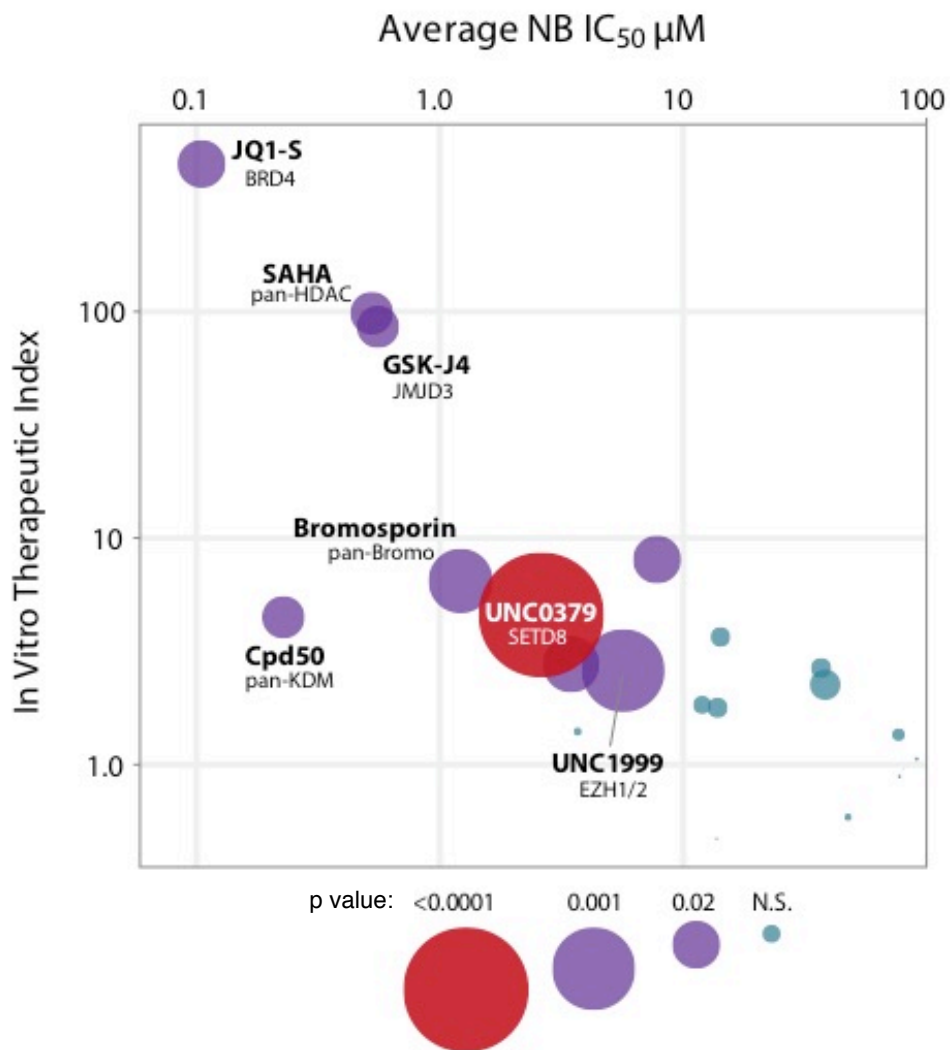


Figure S2, related to Figure 2

Chemical screen of 21 epigenetic probes in NB and normal cells

Bubble graph showing IC₅₀, IVTI and p value of 21 epigenetic probes used in the chemical screen across 8 NB cell lines compared to control cells. The size of the bubble indicates the relative p value calculated by Student's t test.

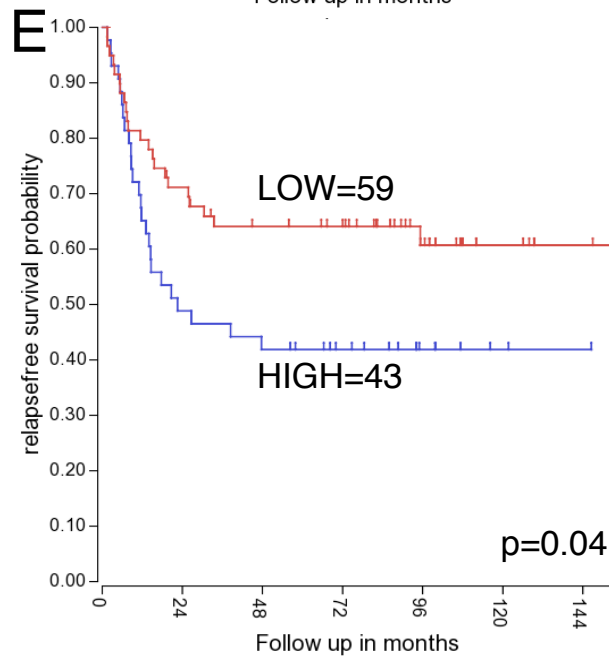
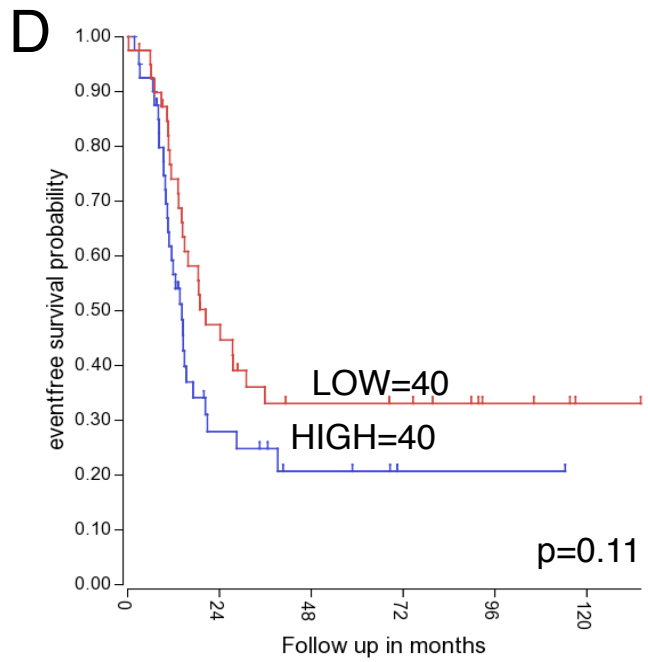
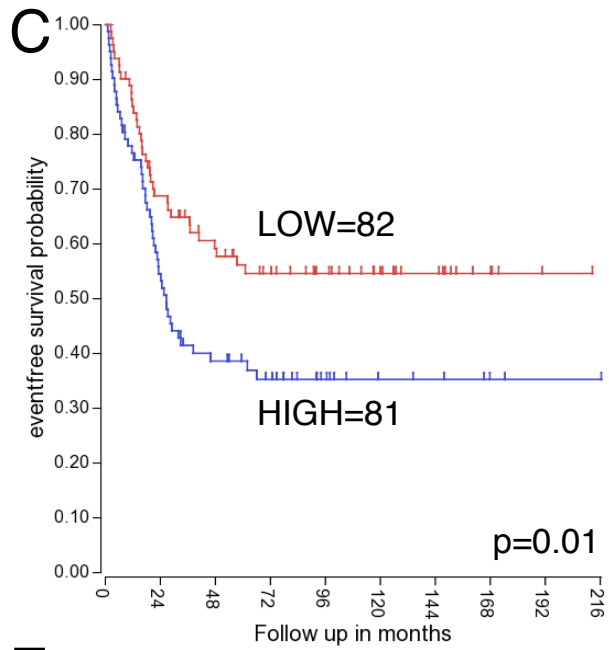
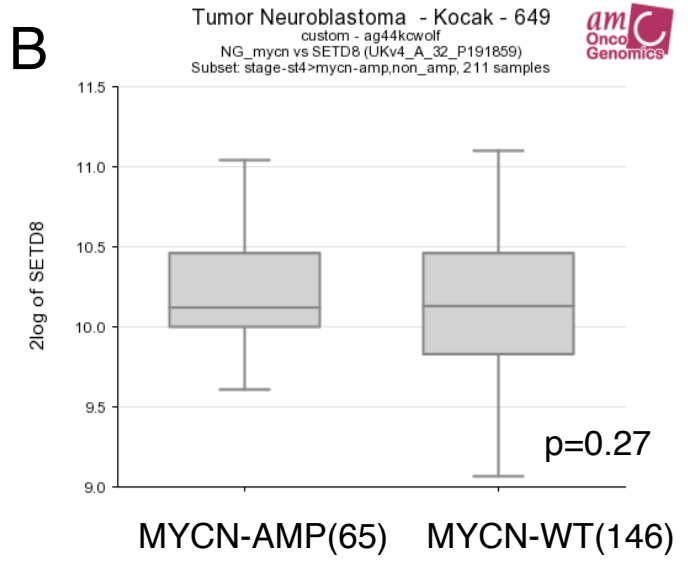
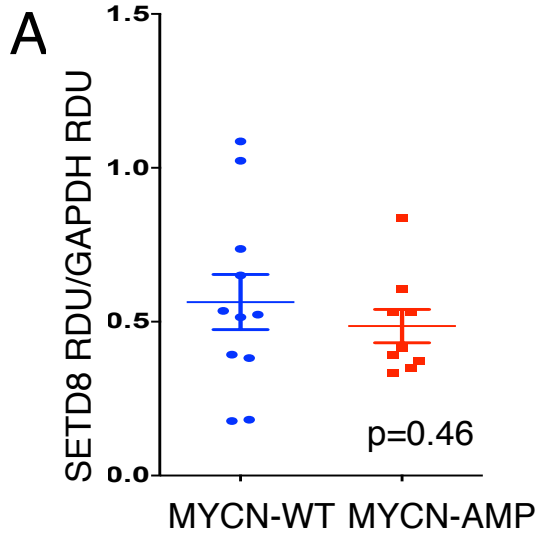


Figure S3, related to Figure 3

SETD8 expression correlates with neuroblastoma prognosis but not with MYCN status in vitro

(A) Densitometric analysis of SETD8 protein levels normalized on GAPDH protein levels in 14 NB cell lines calculated as RDU (Relative Densitometric Unit) ($p=0.46$). Symbols indicate individual cell lines ($n=11$ MYCN-WT; $n=9$ MYCN-amp). Bars show average \pm SEM. p value was estimated by two-tailed Student t test. (B) Box Plot showing that levels of SETD8 mRNA in Stage 4 MYCN-WT and MYCN amplified NB tumors (R2 database: Kocak $n=476$, stage4-NB tumors, $p=0.27$). (C-E) Kaplan-Meier graphs stratified by expression of SETD8 in MYCN-WT or MYCN amplified stage 3 and 4 NB patient tumors (R2 database: SEQC-498-RPMseqcnb1-stage3,4 $p = 0.01$ (C), SEQC-498-RPM-seqcnb1- stage3,4 $p = 0.11$ (D) and non MYCN ampl-Seegeer-102- stage3,4 $p = 0.04$ (E)).

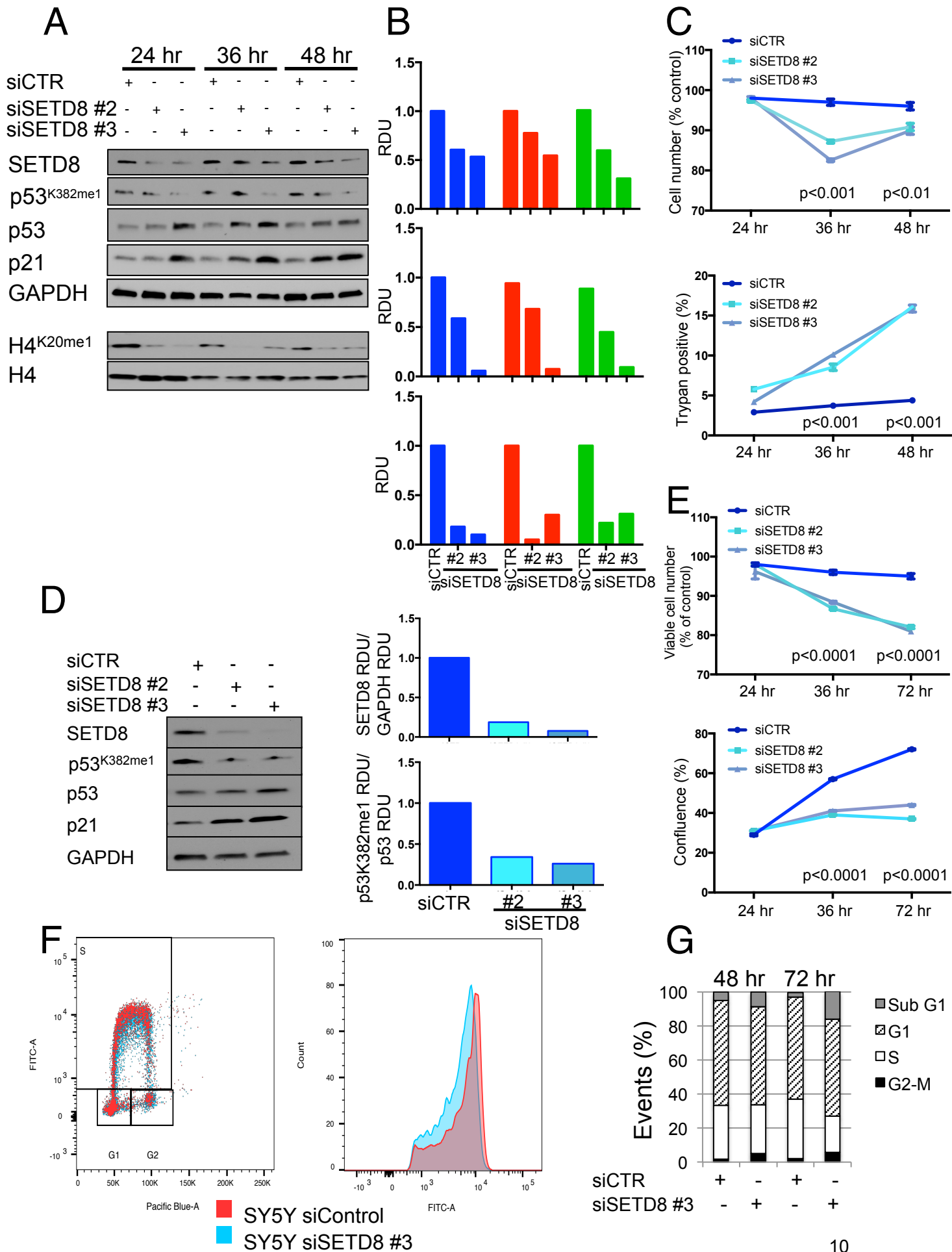


Figure S4, related to Figure 4**Genetic inhibition of SETD8 induces cell growth arrest and apoptotic response through activation of p53 functions**

(A) Time course of SETD8 silencing with 2 different siRNAs at indicated times in SY5Y cells. (B) Densitometric analysis of SETD8 protein levels normalized to GAPDH (upper panel), of p53^{K382me1} protein levels normalized to p53 (middle panel) and of H4K20me1 protein levels normalized to H4 (lower panel) after SETD8 silencing calculated as RDU (Relative Densitometric Unit) from Figure S4A using Image J Software at 24 hr (blue), at 36 hr (red) and at 48 hr (green). The time course experiment was performed three times, the results shown are representative. (C) Viable cell number (upper panel) and Trypan blue positive cells (lower panel) were measured after SETD8 silencing in SY5Y cells at indicated time. (D) Immunoblot of proteins from SY5Y cells after SETD8 silencing for 72 hr blotted with antibodies to p53, p53^{K382me1}, p21 and GAPDH (left panel). Densitometric analysis of SETD8 protein levels normalized to GAPDH (upper) and of p53^{K382me1} protein levels normalized to p53 (lower) are depicted in the right panels. (E) Viability and confluence were analyzed 24, 48 and 72 hr after SETD8 silencing. (F) Cell cycle analysis of SY5Y 36 hr after SETD8 silencing: EDU incorporation and the relative level of DNA synthesis per cell after SETD8 silencing (blue) are indicated and compared with control (red). (G) Cell cycle analysis of SY5Y 48 and 72 hr after SETD8 silencing using siSETD8 #3 sequence. Cells were stained with Pacific Blue-A and analyzed by flow cytometry. The data show percentage of events in sub-G1, G1, S, G2-M phase.

Table S5, related to Figure 4 and Figure 5

The top differentially up- and down-regulated genes after SETD8 silencing and UNC0379 treatment ranked by statistical significance based on edgeR software analysis and a false discovery rate (FDR) < 0.001. Provided as an Excel file.

Table S6, related to Figure 4 and Figure 5

p53 downstream pathway gene list in SETD8 genetic and pharmacological inhibition. Provided as an Excel file.

Table S7, related to Figure 4: *FRUMM NB differentiation gene list* enriched in SETD8 genetic inhibition.

PROBE	RANK IN GENE LIST	RANK METRIC SCORE	RUNNING ES	CORE ENRICHMENT
EGR1	148	6.0066	0.0629	Yes
RGS16	158	5.8623	0.1332	Yes
CDKN1A	239	4.6821	0.1846	Yes
PLK2	271	4.2829	0.2344	Yes
DOCK4	566	2.8409	0.2494	Yes
ADD3	603	2.7074	0.2798	Yes
SYT11	948	2.0193	0.2817	Yes
CACNA2D2	1031	1.8896	0.2991	Yes
DPYSL3	1112	1.7715	0.3153	Yes
DLK1	1235	1.5987	0.3266	Yes
ARHGEF3	1288	1.5165	0.3415	Yes
CRABP2	1420	1.4020	0.3499	Yes
VGF	1553	1.3327	0.3574	Yes
CHST5	2002	1.0000	0.3400	No
GATA3	2647	0.9489	0.3092	No
KCTD13	2862	0.7900	0.3047	No
PLEKHA6	2977	0.7177	0.3059	No
N4BP1	3606	0.4096	0.2697	No
MTMR1	3643	0.3906	0.2720	No
JARID2	4055	0.2329	0.2478	No
HOXD4	4072	0.2231	0.2495	No
HERC2	4212	0.1676	0.2424	No
CTSB	4386	0.0974	0.2322	No
CRH	4825	-0.0554	0.2041	No
ST6GAL1	4931	-0.1026	0.1985	No
ASCL1	5258	-0.2116	0.1796	No
HS2ST1	5996	-0.4699	0.1369	No
STX6	6485	-0.6220	0.1124	No
KCTD12	6711	-0.7116	0.1062	No
CPSF1	7007	-0.8166	0.0967	No
CHGA	7093	-0.8452	0.1014	No
CALML4	7139	-0.8690	0.1089	No
DDAH2	7314	-0.9408	0.1089	No
FLNB	7343	-0.9573	0.1186	No
PTBP1	8316	-1.1258	0.0684	No
MMP11	8544	-1.2173	0.0683	No
SLC29A1	9607	-1.6321	0.0183	No
MAFF	10795	-2.1692	-0.0334	No
PRKCH	11289	-2.4203	-0.0365	No
SYNJ2	12278	-3.0412	-0.0646	No
PPIF	12301	-3.0648	-0.0290	No
RAB20	12577	-3.2960	-0.0072	No
PLAT	12578	-3.2962	0.0327	No
RBP1	13082	-3.8099	0.0457	No
IGFBP5	13315	-4.0412	0.0794	No
TPST1	13341	-4.0764	0.1270	No

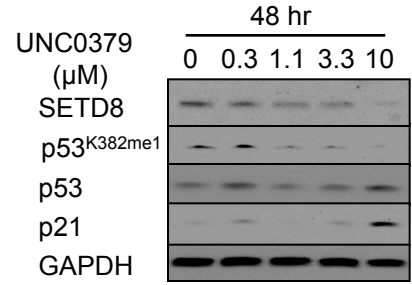
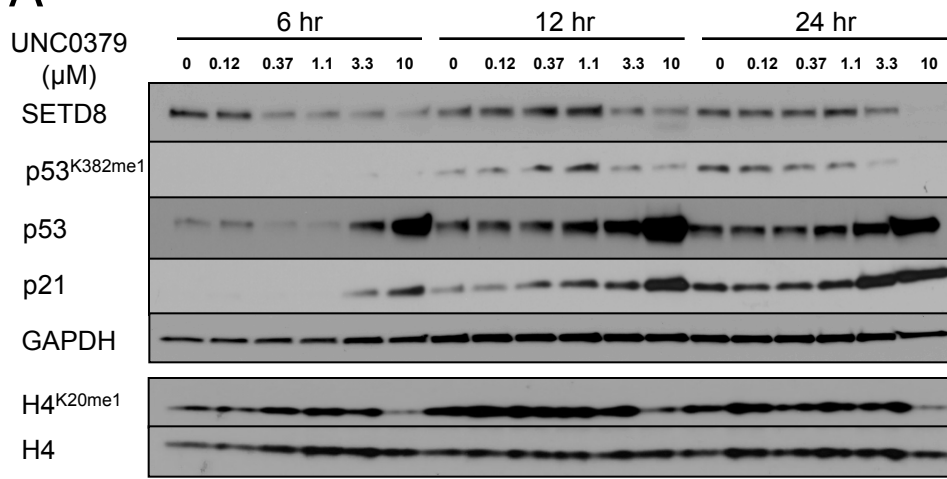
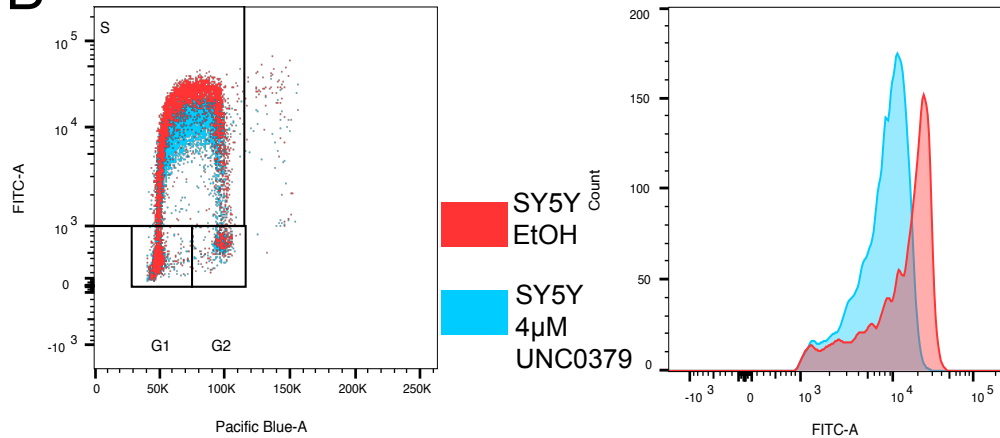
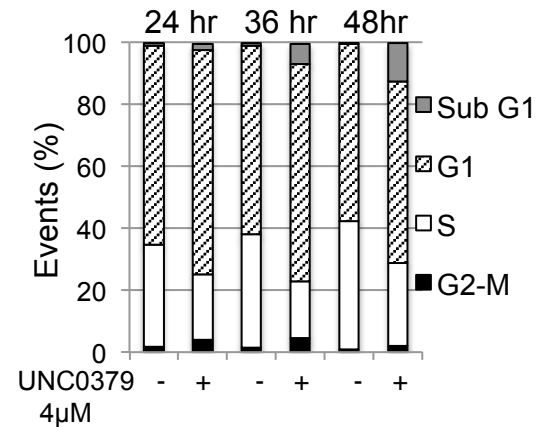
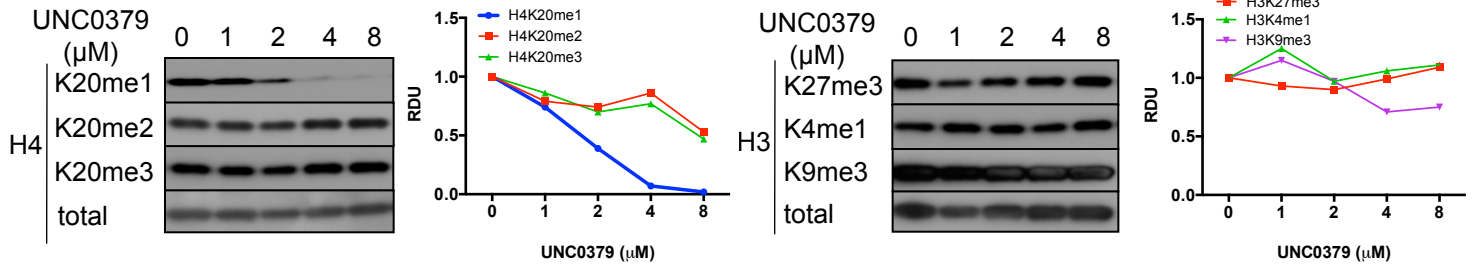
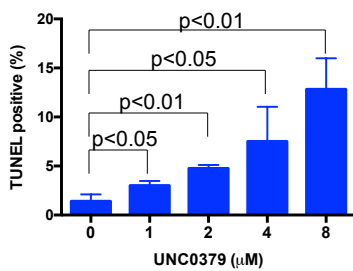
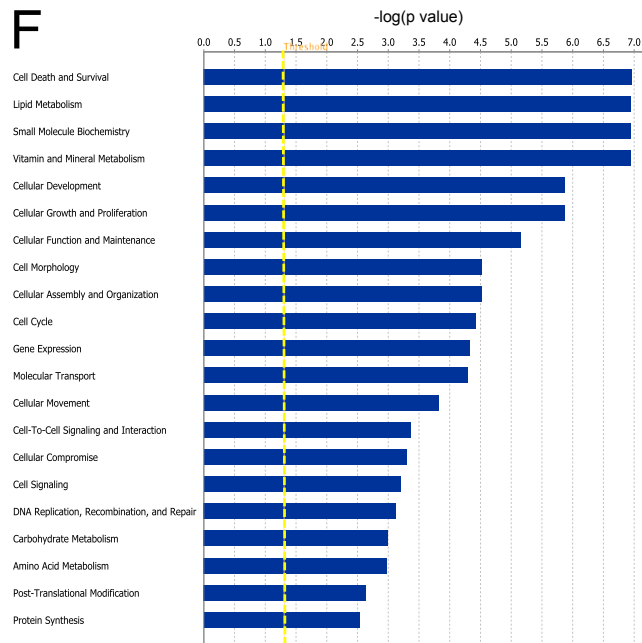
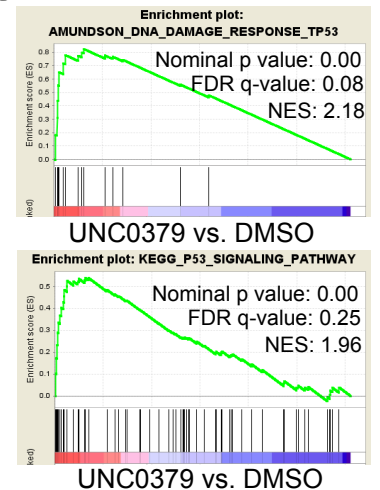
A**B****C****D****E****F****G**

Figure S5, related to Figure 5**Pharmacological inhibition of SETD8 induces growth arrest, apoptosis and activation of p53**

(A) Immunoblot of the indicated proteins from SY5Y cells after UNC0379 treatment at indicated time and doses. (B) Cell cycle analysis of SY5Y 12 hr after treatment with UNC0379: EDU incorporation and the relative level of DNA synthesis per cell after SETD8 pharmacological inhibition (blue) are indicated and compared to control (red). (C) Cell cycle analysis of SY5Y 24, 36 and 48 hr after treatment with 4 μ M UNC0379. The cells were stained with Pacific Blue-A and analyzed by flow cytometry. The data show percentage of events in sub-G1, G1, S, G2-M phase. (D) Immunoblots of the indicated methyltransferases in SY5Y cells after UNC0379 treatment for 12 hr. Densitometric analysis of the indicated protein levels normalized to total H4 (left panel) and to total H3 (right panel) calculated as RDU (Relative Densitometric Unit) using Image J Software. (E) TUNEL positive cells were measured after UNC0379 treatment for 12 hr in SY5Y cells. Bars show the average of 3 replicates \pm SD. (F) Molecular and cellular functions after UNC0379 treatment (IPA). (G) GSEA of the Amundson DNA damage response p53 pathway (Nominal p value=0.00, FDR=0.08, NES=2.18) and the Kegg p53 signaling pathway (Nominal p value=0.00, FDR=0.25, NES=1.96) after pharmacological inhibition of SETD8.

Table S5, related to Figure 4 and Figure 5

The top differentially up- and down-regulated genes after SETD8 silencing and UNC0379 treatment ranked by statistical significance based on edgeR software analysis and a false discovery rate (FDR) < 0.001.

Table S6, related to Figure 4 and Figure 5

p53 downstream pathway gene list in SETD8 genetic and pharmacological inhibition. Provided as an Excel file.

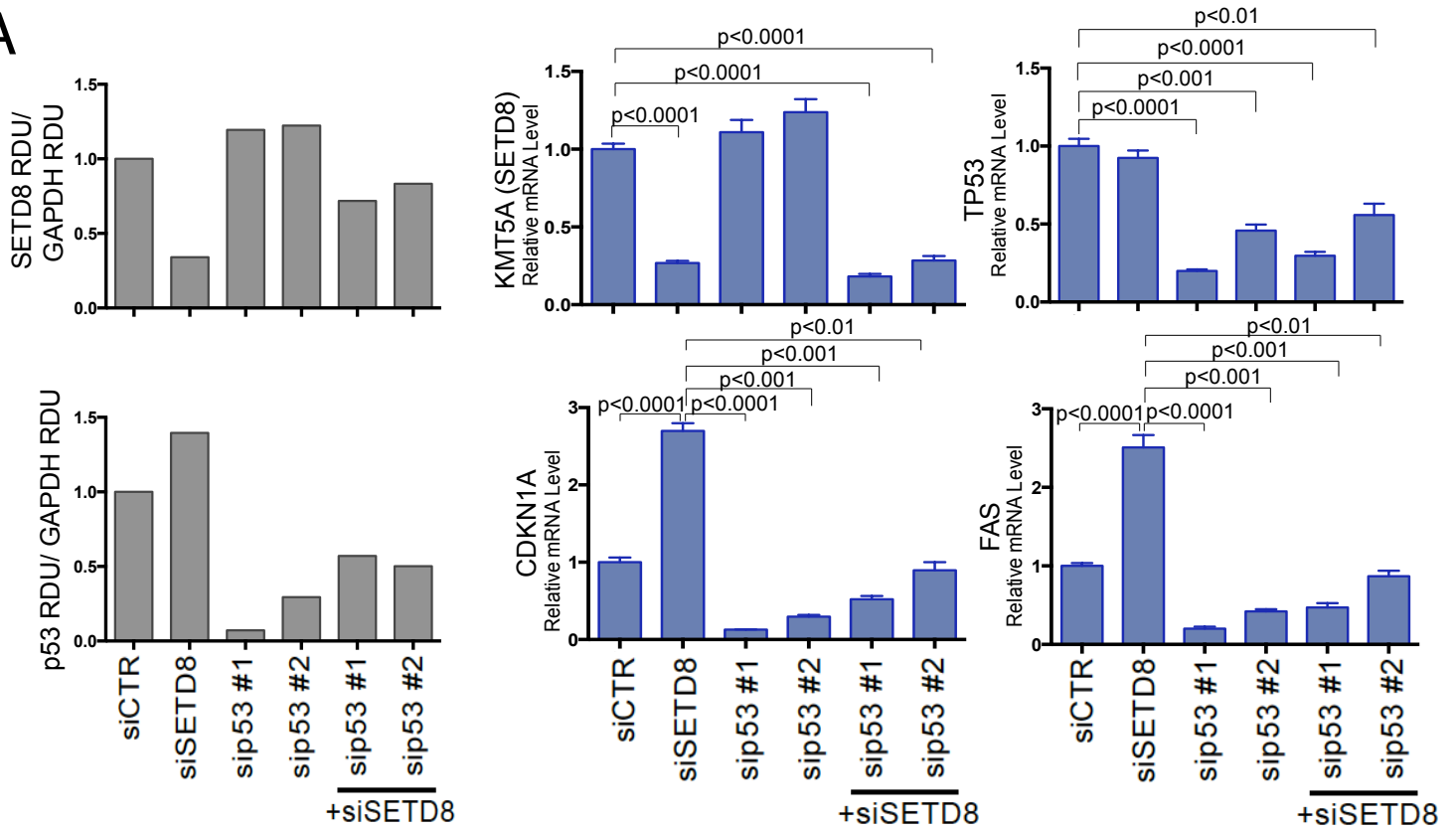
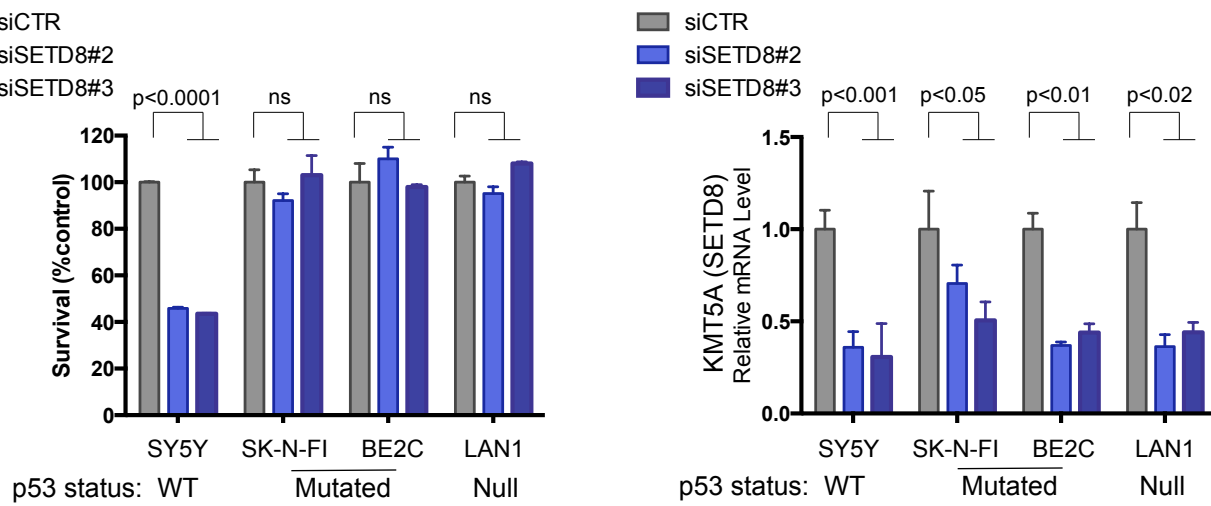
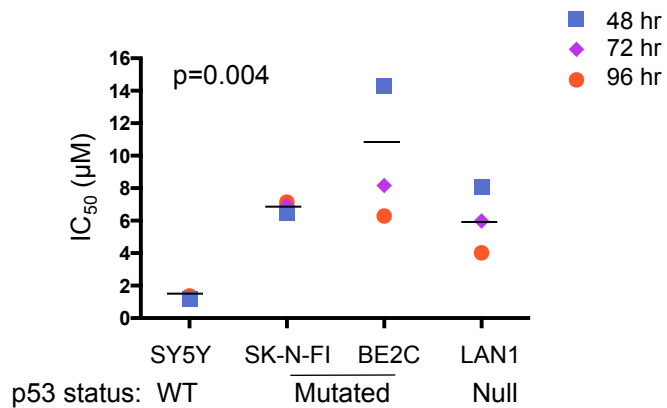
A**B****C**

Figure S6, related to Figure 6

SETD8 silencing induces cell death p53 dependent

(A) Densitometric analysis of SETD8 protein levels normalized on GAPDH (upper left panel) and of p53 protein levels normalized to GAPDH (lower left panel) after SETD8 silencing alone or in combination with p53 silencing shown in Figure 6A calculated as RDU (Relative Densitometric Unit) using Image J Software. qRT-PCR analysis showing the expression of the indicated genes after SETD8 silencing alone or in combination with p53 silencing shown in Figure 6A (upper and lower, middle and right panels, blue graphs). Bars show the average of 3 replicates \pm SEM. (B) MTS assay measured the viability after SETD8 silencing in p53 WT cells (SY5Y), in p53 mutated and null NB cells (SK-N-FI, BE2C and LAN1). Bars show the average of 3 replicates \pm SD (left panel). qRT-PCR analysis showing SETD8 relative mRNA levels after SETD8 silencing in the indicated NB cells. Bars show the average of 3 replicates \pm SEM (right panel). (C) The average IC_{50} was calculated based on the cell confluence values of 3 biological replicates in the indicated NB cell lines at the indicated times (average of 3 biological replicates).

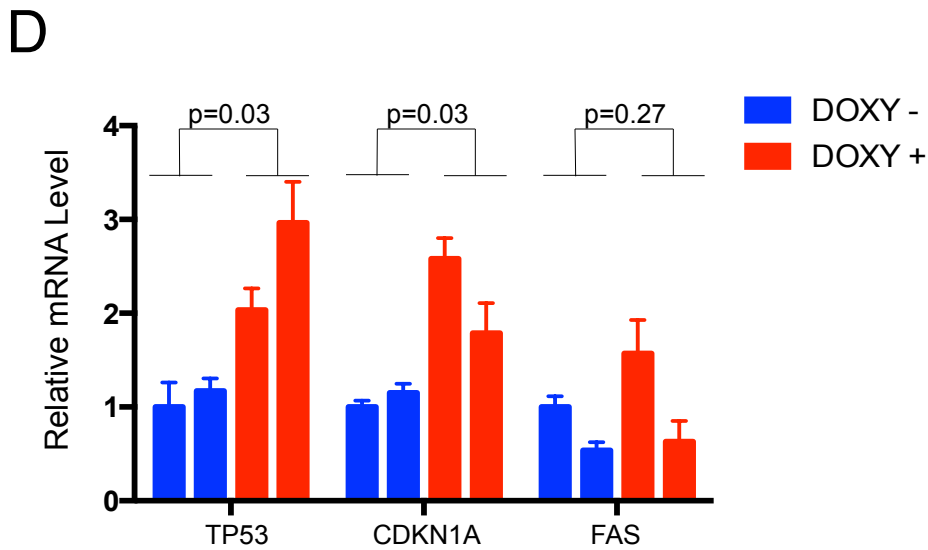
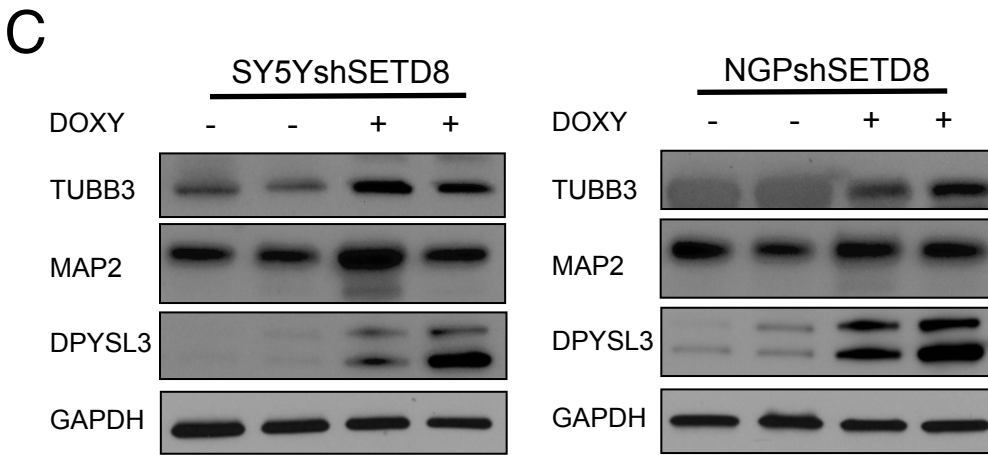
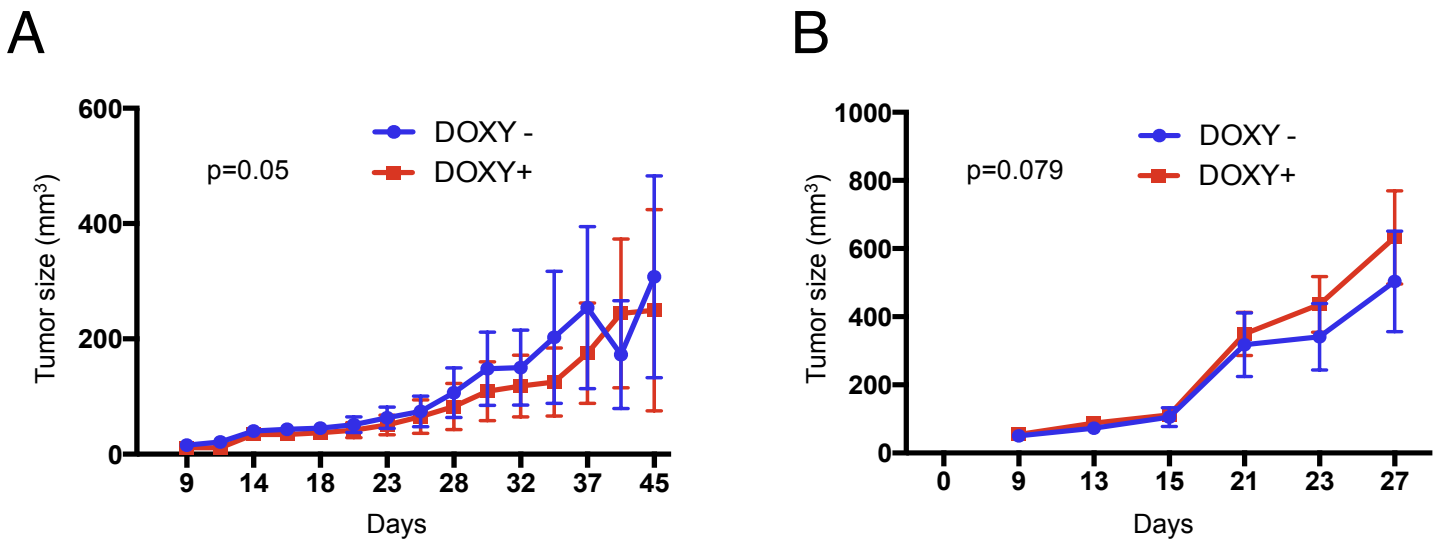


Figure S7, related to Figure 7

Testing the genetic and pharmacological inhibition of SETD8 in neuroblastoma in vivo model

(A-B) Tumor size was evaluated after doxycycline treatment in SY5Y-NB (A) and NGP-NB (B) xenografts derived from cells transfected with empty vector (TRIPZ non-targeted shRNA). Bars show the average tumor size \pm SEM (15 mice/group). Slopes of the growth rate were compared by t test. (C) Immunoblots showing the expression of the indicated neural differentiation markers after genetic inhibition of SETD8 in SY5Y-NB (left panel) and NGP-NB (right panel) xenograft protein extracts in 8 mice randomly chosen from the two groups (untreated and doxycycline-treated). (D) qRT-PCR analysis showing relative mRNA levels of the indicated genes after SETD8 genetic inhibition in 4 mice randomly chosen from the two groups (untreated and doxycycline-treated) 20 days after the injection. Bars show the average of 3 replicates \pm SEM.

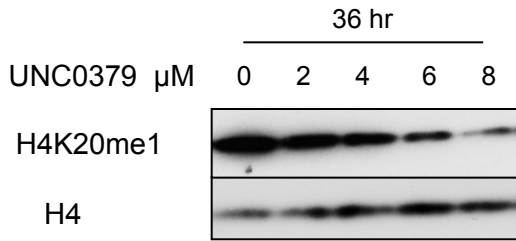
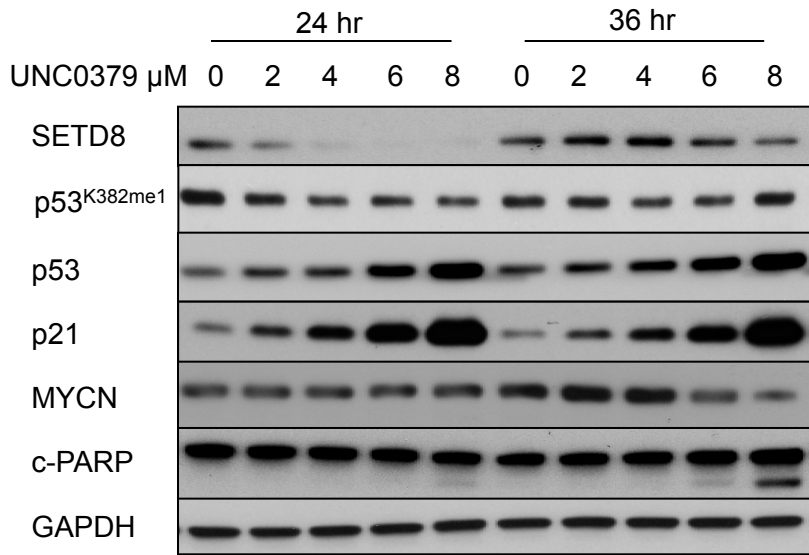
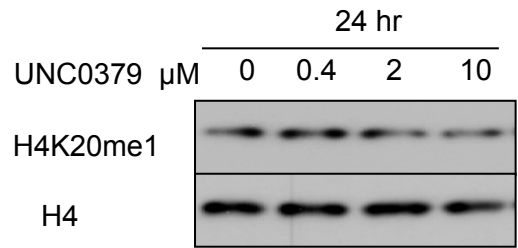
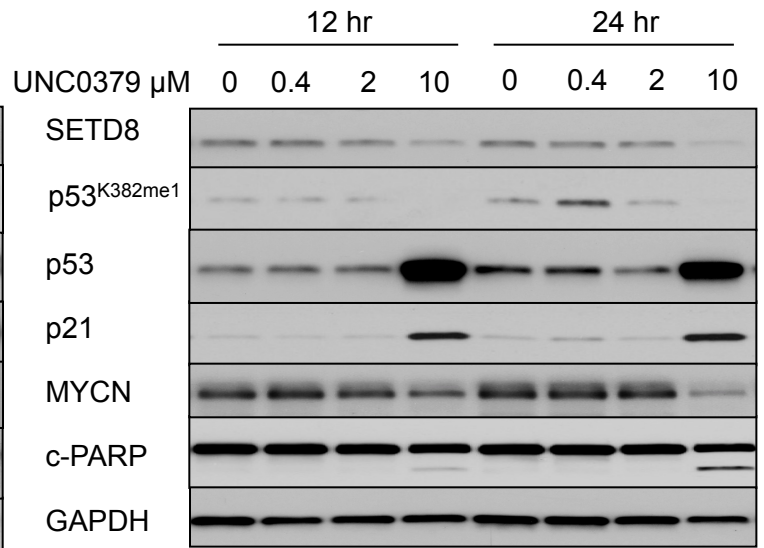
A**B**

Figure S8, related to Figure 5

Pharmacological inhibition of SETD8 in MYCN-amplified neuroblastoma cells

(A-B) Immunoblots of proteins from NGP (A) and IMR32 (B) NB cells after pharmacological inhibition of SETD8 (UNC0379) at indicated time and doses.

SUPPLEMENTAL EXPERIMENTAL PROCEDURES

Cell lines. Eleven human MYCN-WT neuroblastoma (NB) cell lines (SK-N-AS (AS), SK-N-FI (FI), SH-SY5Y (SY5Y), SHEP, SHIN, SK-N-SH, NBLS, NBEB, GICAN, NB16, NB69) and ten human MYCN amplified NB cell lines (SK-N-BE2C (BE2C), LAN1, LAN5, SMS-KCNR (KCNR), IMR32, SMS-SAN (SAN), NB5, NB10, NB19, NGP) were used in this study. NB cell lines were obtained from the cell line bank of the Pediatric Oncology Branch of the National Cancer Institute and have been genetically verified. NB cells were cultured in RPMI-1640 medium supplemented with 10% FBS, 2 mM L-glutamine, 100 µg/mL of penicillin/streptomycin at 37 °C in 5% CO₂. ARPE-19 (human retinal pigment epithelial cell line), HEK293T (human embryonic kidney cell line), C2C12 (mouse muscle myoblast cell line) and NIH3T3 (mouse embryonic fibroblast cell line) were obtained from the ATCC and cultured in DMEM/F12 with 10% fetal bovine serum. MCF 10A (human breast epithelial cell line) were obtained from the ATCC and cultured in MEBM with the additives obtained as a kit: MEGM (Lonza/Clonetics Corporation, Walkersville, MD, USA). Cell cultures were tested and found to be mycoplasma-free.

Reagents. Subconfluent cells were treated with 5 µM all trans retinoic acid (Sigma-Aldrich, St. Louis, MO, USA) for 72 hr or with SETD8 inhibitor, UNC0379 (kindly provided by Jian Jin), at various concentrations for the indicated times. For cell survival assays, SY5Y cells were pretreated with 10µM Z-VAD-FMK (Promega Corporation, Madison, WI) for 3 hr, followed by treatment with 10µM UNC0379 for 48 hr, or treated with UNC0379 or Z-VAD alone for 48 hr. The MTS assay (Promega) was used to detect cell survival according to the manufacturer's instruction. For p53 stability assay upon SETD8 genetic inhibition for 72 hr, SY5Y cells were treated with 50 µg/ml Cycloheximide (CHX) (Cell Signaling, Danvers, MA, USA) for 5, 10, 15, 20, 30, 60 min. Linear regression analysis (one-phase exponential decay) of the p53 half-life after SETD8 silencing and CHX treatment was performed. SETD8 inhibition increased p53 half-life approximately 10 fold (siCTR: K=0.182, half-life=3.8 min; siSETD8: K=0.0176, half-life=39.5 min).

Caspase-Glo 3/7 assay. Subconfluent cells were plated on multiwell 96 plate. After treatment with the indicated concentrations of UNC0379 or SETD8 silencing or p53 overexpression, caspase-3/7 activities were detected using a Caspase-Glo 3/7 Assay (Promega) according to the manufacturer's instruction. Luminescence of each sample was measured in a plate-reading luminometer VICTOR 3 (PerkinElmer, Waltham, MA, USA). The experiment was performed in duplicates and repeated three times.

TUNEL assay. Subconfluent cells were plated on 8 well chamber slide and treated with the indicated concentrations of UNC0379 or silenced for SETD8 expression at the indicated times. Terminal deoxynucleotidyl transferase-dUTP nick end labeling (TUNEL) assay was performed using a Click-iT Plus TUNEL Assay (Thermo Fisher Scientific, Waltham, MA, USA) according to the manufacturer's instruction. TUNEL positive cells were examined under a fluorescence microscope (Nikon TE2000). At least 200 cells/sample were counted. The experiment was performed in duplicates and repeated three times.

Transfection, transduction and constructs. SY5Y cells were plated on 100-mm dishes at a density of 5×10^6 cells per dish. After 24 hr cells were infected by SETD8 or non-target short hairpin RNA (shRNA) TRIPZ lentiviral inducible particles (GE Healthcare, Little Chalfont, Buckinghamshire, UK) following the manufacturer's protocol.

NGP cells were transfected by electroporation with Nucleofector Solution V, in a Nucleofector II device (Amaxa Biosystems, Gaithersburg, MD, USA). For stable integration, NGP cells were transfected with a tetracycline (TET) inducible TRIPZ shSETD8 vector (RHS 4696-200678840) (GE Healthcare) and selected in the presence of 500 µg/ml puromycin (Sigma-Aldrich) and then treated with or without 1µg/ml doxycycline (DOX).

LAN1 cells were transfected with p53 WT and p53K382R mutant vectors (described previously (Shi et al., 2007)) using Lipofectamine 2000 reagent (Invitrogen) according to the manufacturer's instructions. After 24 hr cells were treated with or without 8 µM UNC0379 for 24 hr. The empty pCAG3.1 vector was used as mock control.

siRNA-mediated knockdown of SETD8 and p53. SETD8 knockdown was obtained by transfection of SY5Y, SK-N-FI, SK-N-BE2C and LAN1 cells for 72 hr with two Dharmacon on-target plus siRNAs targeting human SETD8 (5'-GCAACUAGAGAGACAAAUC-3'/5'-GAUUGAAAGUGGGAAGGAA-3') using Lipofectamine 2000 reagent (Invitrogen) according to the manufacturer's instructions. p53 knockdown alone or in combination with SETD8 knockdown was obtained by transfection of SY5Y cells for 48 hr with two Dharmacon on-target plus p53 siRNAs (5'-GAAUUUGCGUGUGGAGUAUU-3'/5'-GUGCAGCUGUGGGUUGAUUUU-3') using Lipofectamine 2000 reagent (Invitrogen) according to the manufacturer's instructions. On-target plus non-targeting siRNA (5'-UGGUUUACAUGUCGACUAA-3', Dharmacon) was used as a control.

Cell cycle analysis. Cell cycle analysis of SY5Y was performed after SETD8 silencing or treatment with 4 μ M UNC0379 at the indicated time. For S phase analysis, cells were stained using Click-iT® EdU Alexa Fluor® 488 Flow Cytometry Assay Kit (Thermo Fisher Scientific, Waltham, MA, USA) according to the manufacturer's instructions. The cells were counterstained with FxCycle™ Violet Stain (Thermo Fisher Scientific) and analyzed by flow cytometry (BD FACSCanto II, BD Biosciences). For each sample 20000 events were collected. Three biological replicates were performed and representative data are shown.

For M-phase quantification in human cell lines, cells were incubated in Alexa Fluor 488-conjugated mouse anti-phospho H3 (Ser10, Clone 3H10, human specific) antibody (Millipore, Cat. FCMA104A4, 1:50) in 100 μ l 1x Click-iT saponin-based permeabilization and wash buffer (Life Technologies) overnight at 4°C. For M-phase quantification in murine cell lines, cells were incubated in anti-phospho H3 (Ser10) antibody (abcam Cat. ab14955, 1:50) in 100 μ l 1x Click-iT saponin-based permeabilization and wash buffer overnight at 4°C. Cells were washed once and incubated in FITC-conjugated goat anti-mouse IgG (Santa Cruz, Cat. sc-2010, 1:100) in 100 μ l 1x Click-iT saponin-based permeabilization and wash buffer. Stained human and murine cell lines were washed once and resuspended in 0.5ml of 1 μ g/ml FxCycle Violet (Life Technologies Cat. F10347) in 1x Click-iT saponin-based permeabilization and wash buffer for DNA content staining. Cells were stained for 30 min at room temperature prior to flow cytometry.

Indirect immunofluorescent cytochemical staining. Subconfluent cells were plated on 8 well chamber slide and treated with UNC0379 4 μ M or transfected with siSETD8 for 72 hr. Indirect immunofluorescence was used to study the expression of TUBB3 (β -tubulinIII), MAP2 and DPYSL3 in SY5Y. Cells were fixed in 4% formaldehyde/PBS for 15 min, permeabilized in 0.25% Triton/PBS for 10 min, blocked by incubation with 5% goat serum in PBS containing 0.1% Triton X-100 for 1 hr RT, and incubated o/n with primary Abs, mouse anti-TUBB3 (β -tubulinIII), dilution 1:250 (Millipore, Billerica, MA, USA); rabbit polyclonal anti-DPYSL3 dilution 1:500 (described previously (Tan et al., 2013)); mouse anti-MAP2 dilution 1:100 (Santa Cruz Biotechnology, Santa Cruz, CA, USA), followed by secondary FITC-conjugated species-specific antisera dilution 1:250 (Invitrogen). DAPI was added at a dilution 1:10000 (Invitrogen). Increased expression of these three neural differentiation markers, TUBB3 (β -tubulinIII), MAP2 and DPYSL3, was detected upon genetic and pharmacologic SETD8 inhibition. Representative images of TUBB3 (β -tubulinIII), expression are shown.

Western blotting. Cells were washed 3x in cold PBS, mechanically detached and the cell suspension divided in two with one harvested for total proteins and the other subjected to a histone protein extraction. Total protein extracts were obtained in RIPA buffer (50 mM Tris pH 8, 150 mM NaCl, 0.5% sodium deoxycholate, 0.1% SDS, 1% NP40, 1 mM EDTA and a mix of protease inhibitors). Total histone extracts were prepared using the EpiQuick Total Histone Extraction Kit according to the manufacturer's protocol (Epigentek, Farmingdale, NY, USA).

Total protein extracts (30 μ g/sample) and histone extracts (2 μ g/sample) were separated by SDS-PAGE and blotted onto nitrocellulose membranes (PerkinElmer, Waltham, MA, USA). Membranes were blocked with 5% nonfat dry milk and incubated with primary antibodies (Abs) at the appropriate dilutions. The following Abs were used: mouse anti-p53 (DO-I), mouse anti-MYCN, mouse anti-MAP2, rabbit polyclonal anti-GAPDH and rabbit polyclonal anti-p21 (Santa Cruz Biotechnology, Santa Cruz, CA, USA); mouse anti-SETD8 (Abcam Inc, Cambridge, MA, USA), mouse anti-TUBB3 (β -tubulinIII), and rabbit polyclonal anti-H3K27me3 (Millipore, Billerica, MA, USA); rabbit polyclonal anti-H3, rabbit polyclonal anti-H3K4me1, rabbit polyclonal anti-H4, mouse anti-H3K9me3, mouse anti-H4K20me1, mouse anti-H4K20me2 and mouse anti-H4K20me3 (Active Motif, Carlsbad, CA, USA); rabbit polyclonal anti-PARP (Cell Signaling, Danvers, MA, USA), rabbit polyclonal anti-p53K382me1 (described previously (Shi et al., 2007)); rabbit

polyclonal anti-DPYSL3 (described previously (Tan et al., 2013)). Immunoreactive bands were visualized by enhanced chemoluminescence (Perkin Elmer). ECL signals were detected using film or Imager and were quantified using the Imager. Densitometry analysis was performed and measured as RDU (relative densitometric units) using Image J Software. All experiments were performed at least three times. The western blots shown are representative and associated densitometric analysis refer to the blots shown.

Real-Time PCR analysis

Total RNA extraction was carried out using an RNeasy Plus Kit (Qiagen Inc., Hilden, Germany) and quantitative reverse transcription-PCR (qRT-PCR) was performed as described (Veschi et al., 2014). Primer sequences were as follows: SETD8-forward 5'-ACTTACGGATTTCTACCCTGTC-3', SETD8-reverse 5'-CGATGAGGTCAATCTTCATTCC-3'; p21-forward 5'-GGCAGACCAGCATGACAGATT-3', p21-reverse 5'-GCGGATTAGGGCTTCCTCTT-3'; p53-forward 5'-GCCCCACTTCACCGTACTAA-3', p53-reverse 5'-TGGTTTCAAGGCCAGATGT-3'; BAX-forward 5'-GGGACGAAGTGGACAGTAACA-3', BAX-reverse 5'-CCGCCACAAAGATGGTCAC-3'; FAS-forward 5'-TGAAGGACATGGCTTAGAAGTG-3', FAS-reverse 5'-GGTGCAAGGGTCACAGTGTT-3'; MDM2-forward 5'-CATTGAACCTTGTGTGATTTGTC-3', MDM2-reverse 5'-GCAGGGCTTATCCTTTTCTTTA-3'; HPRT-forward 5'-TGACACTGGCAAACAATGCA-3', HPRT-reverse 5'-GGTCCTTTTACCAGCAAGCT-3'. All amplification reactions were performed in triplicates and data were normalized to the housekeeping gene HPRT.

siRNA transfection in a 384-well format and automated imaging. Cells used for this screening were BE2C and SY5Y stably transfected with GFP. Cells were transfected in quadruplicate (2 biological replicates, SY5Y; 1 biological replicate, BE2C) with siRNA oligos at a final concentration of 50 nM in a reverse format using a Janus automated liquid handler (Perkin-Elmer). First, 3.75 μ l of OPTIMEM (Invitrogen) were transferred into each well of an empty PE-Cell Carrier 384-well imaging plate (Perkin-Elmer). Then, 1.25 μ l of a 1 μ M siRNA stock was added to the well. Finally, 5 μ l of Lipofectamine 2000 diluted in OPTIMEM was added to the siRNA. Plates were incubated for 20 min at RT and then 5000 cells/well were seeded in the plate in a 20 μ l volume of RPMI medium, 20% FBS, 100 U/ml penicillin and 100 μ g/ml streptomycin using a Multidrop Combi automated dispenser (Thermo Fisher Scientific). The influence of possible edge effects was limited by not using columns 1 and 24 and rows A and P of the assay 384-well plate. The edge rows/columns were seeded with cells but were not used for the experiment. Cells were incubated at 37 °C for 72 hr.

Fixation, washing and staining steps were performed using a Biotek EL406 automated plate washer/dispenser. Cells were fixed and stained by adding 25 μ l/well of 4% paraformaldehyde with Hoechst 33342 (1 μ g/ml) in PBS directly into the culture medium and incubated for 15 min at RT. The automated imaging steps were performed using an Opera high-throughput confocal microscope (PerkinElmer). A 20 \times water objective was used for image acquisition. Images were acquired in 12 randomly selected fields of view per well, five z-planes (1 μ m apart) by using a 405 nm excitation laser (1st acquisition) and then using a 488 nm excitation laser (2nd acquisition). Images were analyzed using the Columbus image analysis server (Perkin-Elmer). Typically, >300 cells were imaged per well. The Z-factor of this assay is 0.561. Columbus quantified two parameters: cell proliferation (Nuclei Number) and differentiation (Neurite Length) (Wang et al., 2010) (Yang et al., 2013). Neurite length was calculated as the average neurite length per field (Figure 1A). For both the primary and secondary screenings, we used an siRNA that induced cell death as a positive control for changes in NN, and treatment with 5 μ M all trans-retinoic acid (RA) as a positive control for changes in NL. We used a non-targeting siRNA pool as a negative control for each replicate. SY5Y and SK-N-BE2C reversed transfected with the positive control cell death siRNA showed 30% or 44% reduction in NN, respectively. The two cell lines treated with RA showed a 30% - 35% increase in NL (Figure S1E). As CENPE, already established as a NB target (Balamuth et al., 2010), met both these parameters in both cell lines, it was used as a positive control in subsequent assays.

Validation of primary hits. The top 16 genes that inhibited NN and increased NL were found in both the replicates. There are no outliers in R1 and R2 data which have the similar distribution (Pearson correlation coefficient and p value: SY5Y-NN $r=0.46$, $p<0.0001$ (Figure S1A, left graph); SY5Y-NL $r=0.56$, $p<0.0001$ (Figure S1B, left graph); BE2C-NN $r=0.26$, $p<0.0001$ (Figure S1C, left graph); BE2C-NL $r=0.38$, $p<0.0001$ (Figure S1D, left graph)).

A permutation test was performed for each data set (SY5Y_NN, SY5Y_NL, BE2C_NN, BE2C_NL) using linear model (linear model function in R) resampling 300 genes from the data 1000 times. The mean and standard deviation of t value and $-\log_{10}$ p value for SY5Y_NN in the permutation test are 9.0 ± 0.62 (t value \pm SD) and 16.1 ± 1.95 ($-\log_{10}$ p value \pm SD) (Figure S1A, middle and right graphs); for SY5Y_NL, 11.9 ± 0.66 and 25.84 ± 2.33 (Figure S1B, middle and right graphs); for BE2C_NN, 4.68 ± 0.50 and 4.9 ± 1.04 (Figure S1C, middle and right graphs); for BE2C_NL, 7.24 ± 0.54 and 10.95 ± 1.49 (Figure S1D, middle and right graphs). The small variations of t values and significant p values support the robustness of the screen. To minimize false positives due to off-targets effects of the pooled siRNAs, we designed a new Dharmacon library using the smartpool siRNAs as well as their deconvoluted single siRNAs and performed a validation screen. Candidate genes from the initial screen were ranked based on the following criteria: 1) Z-score < 2 or > 2 for nuclei number and/or in neurite length; 2) potential druggability due to enzymatic activity; and 3) prognostic significance in primary neuroblastoma tumor tissues databases (database: R2 Genomics Analysis and Visualization Platform; <http://r2.amc.nl>). From these criteria we selected 12 genes for validation. To validate these genes, we required that at least 50% of the deconvoluted siRNAs resulted in a significant reduction in nuclei number and increase in neurite length compared with controls for both cell lines (Figure 1C).

Chemical screening in a 384-well format and epigenetic drugs. NB and control cell lines were plated in duplicate in 384-well plates at indicated densities (AS, 500 cells; NBEB and NBL5 2500 cells; NGP, 3500 cells; SY5Y, BE2C and KCNR 4000 cells; IMR32, 5000 cells; ARPE-19, 2000 cells; HEK293T, 3000 cells). Twenty-one epigenetic chemical probes (Structural Genomics Consortium), which targeted 90% of the epigenetic enzymes present in the siRNA library, were used in this study. For a complete list of the epigenetic drugs and their targets see Figure 2B. The chemicals were dissolved in DMSO (or 95% ethanol) to a stock concentration of 10 mM and subsequently diluted to the indicated concentrations in cell culture media. After 24 hr, cells were treated and cultured for the indicated time periods. Eight NB cell lines and two normal immortal but non-transformed cell lines were evaluated utilizing 12 doses (0.1-30 μ M) over the course of 7 days. The cell confluency was recorded every 4 hr by IncuCyte Zoom System (Essen BioScience, Ann Arbor, MI, USA). The high-throughput chemical screening was performed three times. The average IC_{50} was calculated based on the cell confluency values of three biological replicates across eight NB cell lines after 96 hours using the software GraphPad Prism 6.0. The In Vitro Therapeutic Index (IVTI) was calculated as the average IC_{50} of the control cell lines divided by the average IC_{50} of NB cell lines.

Sample preparation for RNA-seq. RNA was isolated and subjected to RNA-seq analysis from SY5Y cells 36 hr after siRNA inhibition of SETD8 (using siCTR or siSETD8 #3) and 12 hr after treatment with DMSO or 4 μ M (IC_{80}) UNC0379. Two independent biological replicates were performed in each group (siSETD8 and UNC0379). Total RNA extraction was carried out using an RNeasy Plus Kit (Qiagen Inc., Hilden, Germany) according to the manufacturer's instructions.

Specifically, for SETD8 genetic inhibition, SY5Y cells were transfected with two of the SETD8 siRNAs sequences used in the siRNA screen and evaluated for SETD8 silencing, cell number, viability and cell cycle progression (Figure S4). By 36 hr after siRNA transfection, SETD8 mRNA levels decreased by 80% and the levels of its target H4K20me1 decreased by 90%. Cell numbers decreased by less than 10% at 36 hr, by 15% at 48 hr and by 20% at 72 hr after SETD8 inhibition (Figures S4A-S4E). Although assessment of cell cycle distributions 36 and 48 hr after SETD8 inhibition did not indicate a marked decrease in the number of cells in S-phase, levels of EDU incorporation suggested a decrease in the rate of DNA synthesis per cell (Figure S4F). By 72 hr the S-phase fraction decreased by 40%, the G2-M phase fraction increased by a factor of 3, and the number of cells with sub-G1 DNA content increased by a factor of 5.4 (Figure S4G). Transcriptional changes in SY5Y cells following 36 hr of treatment with SETD8 siRNAs were analyzed by RNA-seq (Illumina). This time was chosen as both histone and non-histone targets were inhibited and effects on cell viability were minimal.

Specifically, for SETD8 pharmacological inhibition, SY5Y were treated with UNC0379 or DMSO and evaluated for target inhibition, cell viability, cell death and cell cycle progression (Figure S5). At 12 hr, there was no change in the percentage of UNC0379-treated cells in S-phase compared with control-treated cells, although EDU labeling indicated a relative decrease in their level of DNA synthesis per cell compared to the controls (Figure S5B). There was a 36-50% decrease in the S-phase fraction from 24-48 hr in the UNC0379-treated cells which was accompanied by a 2 to 28-fold increase in their subG1 fraction

during the same time frame compared to the controls (Figure S5C). Transcriptional changes in SY5Y cells following 12 hr of treatment with 4 μ M UNC0379 were analyzed by RNA-seq (Illumina). This time was chosen as both histone and non-histone targets were inhibited and effects on cell viability were minimal.

Sequencing and alignment. Strand-specific whole transcriptome sequencing libraries were prepared using TruSeq® Stranded Total RNA LT Library Prep Kit (Illumina, San Diego, CA, USA) by following the manufacturer's procedure. This protocol involved the removal of ribosomal RNA (rRNA) using biotinylated, target-specific oligos combined with Ribo-Zero rRNA removal beads. The RNA was fragmented into small pieces and the cleaved RNA fragments were reverse-transcribed to generate first strand cDNA using reverse transcriptase and random primers, followed by second strand cDNA synthesis using DNA Polymerase I and RNase H. The resulting double-strand cDNA was used as the input to a standard Illumina library prep with end-repair, indexed adapter ligation and PCR amplification to generate sequencer-ready libraries. Eight indexed RNA-seq libraries were sequenced on a HiSeq2500 with Illumina TruSeq V4 chemistry (Illumina, San Diego, CA, USA). The Fastq files with 125bp paired-end reads were processed using Trimmomatic (version 0.30) (Bolger et al., 2014) to remove low quality bases. The trimmed fastq data were aligned to human genome hg19 with STAR (version 2.4.2a) (Dobin et al., 2013) which used GENCODE gtf file version 19 (Ensembl 74). STAR software also generated the strand-specific gene read counts. About 77% of 70 million reads per sample were mapped to human genome uniquely for a total of 90% mapping rate.

Differential expression analysis. The gene reads count data from STAR for UNC0379 and siSETD8 samples were analyzed separately with R Package EdgeR (version 3.10.5) (Robinson et al., 2010). EdgeR performed the generalized linear model (GLM) likelihood ratio test to determine genes differentially expressed between any of the groups from each compound. EdgeR was also used to normalize the reads count data to generate z-scores for heatmap display.

Pathway analysis and heatmaps. Statistical results of differentially expressed genes from EdgeR were analyzed using QIAGEN's Ingenuity® Pathway Analysis (IPA®, QIAGEN Redwood City, www.qiagen.com/ingenuity, IPA Fall Release, September 2015). Genes with p values or false discovery rates (FDRs) less than the cutoff were used as input for IPA core analysis which calculated significant canonical pathways and generated pathway figures. Heatmaps for the top 50 up- or down-regulated genes for each compound were created in R using the heatmap.2 function in g plots (version 2.17.0).

In vivo studies. For heterotypic subcutaneous injection, SY5Y and NGP cells were washed with Hanks balanced salt solution (HBSS) (Invitrogen), and re-suspended in HBSS and Matrigel (Trevigen, Gaithersburg, MD, USA). Cell suspension (100 μ l) containing 2×10^6 cells was inoculated into the subcutaneous tissue of the left flank of 5- to 6-week-old female athymic nude mice (Taconic, Germantown, NY) using a 28-gauge needle (Becton Dickinson, Franklin Lakes, NJ). For the ex-vivo pharmacological inhibition of SETD8, SY5Y and NGP cells were treated ex-vivo with 2 μ M UNC0379 or DMSO for 24 hr and then injected into nude mice (10 mice per group). For the in vivo genetic inhibition of SETD8, 30 mice were injected with stably transfected SY5Y-tet-shSETD8 or NGP-tet-shSETD8 cells and divided in 2 groups. Nine days after tumor injection, when tumors reached approximately 75-150 mm³ half the mice received normal chow while the remainder received DOXY-containing chow. Two additional groups of mice (n=20) were injected with stably transfected TRIPZ non target SY5Y or NGP cells and divided in 2 groups of 10 mice to evaluate the effect of doxycycline alone. The dimensions, length (L) and width (W), of the resulting tumors were determined three times per week using a digital caliper, and the tumor volume (mm³) was calculated as $(L \times W^2)/4$. Twenty days after the injection 5 tumors from each group were excised and protein lysates from these were used to assess SETD8 expression and its targets.

Statistical analysis. Statistical analyses were performed using Microsoft Excel, standard two-tailed Student's *t* test and the software GraphPad Prism 6.0. Image J software was used for quantification of selected immunoblots.

Normalized Z-scores values for the Green/Red ratios and the siRNA rank were calculated using the CellHTS2 package (Boutros et al., Genome Biol 2006). The siRNA pools with Z-Score >2 or <2 for nuclei number (NN) or neurite length (NL) were then selected for secondary validation. The Z-factor of the primary screening is 0.561 for both NN and NL.

For all cell survival and confluence assays, each experiment was performed at least three times. Statistical analysis was performed by a standard two-tailed Student's *t* test.

Student's *t* test was also used to compare the tumor volume between the doxycycline or UNC0379 and non-treatment groups and *p* values of <0.05 were considered to be statistically significant. A paired *t*-test was used to compare the slopes of the growth rates. The analyses were carried out using the software GraphPad Prism 6.0.

The Kaplan-Meier method was used to determine the probability of mice survival as a function of time. The statistical significance between two treatment groups was evaluated using a log-rank test (Mantel-Cox). All *p* values of <0.05 were considered to be statistically significant. The analyses were carried out using the software GraphPad Prism 6.0.

SUPPLEMENTAL REFERENCES

Bolger, A. M., Lohse, M., and Usadel, B. (2014). Trimmomatic: a flexible trimmer for Illumina sequence data. *Bioinformatics* *30*, 2114-2120.

Boutros, M., Bras, L. P., and Huber, W. (2006). Analysis of cell-based RNAi screens. *Genome Biol* *7*, R66.

Dobin, A., Davis, C. A., Schlesinger, F., Drenkow, J., Zaleski, C., Jha, S., Batut, P., Chaisson, M., and Gingeras, T. R. (2013). STAR: ultrafast universal RNA-seq aligner. *Bioinformatics* *29*, 15-21.

Robinson, M. D., McCarthy, D. J., and Smyth, G. K. (2010). edgeR: a Bioconductor package for differential expression analysis of digital gene expression data. *Bioinformatics* *26*, 139-140.

Tan F., Wahdan-Alaswad R., Yan S., Thiele C. J. and Li Z. (2013). Dihydropyrimidinase-like protein 3 expression is negatively regulated by MYCN and associated with clinical outcome in neuroblastoma. *Cancer Sci* *104*, 1586-1592.

Yang, Y. M., Gupta, S. K., Kim, K. J., Powers, B. E., Cerqueira, A., Wainger, B. J., Ngo, H. D., Rosowski, K. A., Schein, P. A., Ackeifi, C. A., *et al.* (2013). A small molecule screen in stem-cell-derived motor neurons identifies a kinase inhibitor as a candidate therapeutic for ALS. *Cell Stem Cell* *12*, 713-726.

Wang D., Lagerstrom R., Sun C., Bishof L., Valotton P. and Götte M. (2010). HCA-vision: Automated neurite outgrowth analysis. *J Biomol Screen* *15*, 1165-70.